Influence of Tryptophan on Lipid Binding of Linear Amphipathic Cationic Antimicrobial Peptides†

Yi Jin,‡ Henriette Mozsolits,§ Janet Hammer,|| Erik Zmuda,|| Fang Zhu,‡,⊥ Yu Zhang,‡,⊥ Marie Isabel Aguilar,§ and Jack Blazyk*,‡,||,⊥

Department of Biomedical Sciences, College of Osteopathic Medicine, Ohio University, Athens, Ohio 45701, Department of Chemistry and Biochemistry and Molecular and Cellular Biology Program, College of Arts and Sciences, Ohio University, Athens, Ohio 45701, and Department of Biochemistry and Molecular Biology, Monash University, Victoria 3800, Australia

Received February 28, 2003; Revised Manuscript Received May 19, 2003

ABSTRACT: We recently demonstrated that a linear 18-residue peptide, $(KIGAKI)_3$-NH_2, designed to form amphipathic β-sheet structure when bound to lipid bilayers, possessed potent antimicrobial activity and low hemolytic activity. The ability of $(KIGAKI)_3$-NH_2 to induce leakage from lipid vesicles was compared to that of the amphipathic α-helical peptide, $(KIAGKIA)_3$-NH_2, which had equivalent antimicrobial activity. Significantly, the lytic properties of $(KIGAKI)_3$-NH_2 were enhanced for mixed acidic−neutral lipid vesicles containing phosphatidylethanolamine instead of phosphatidylcholine as the neutral component, while the potency of $(KIAGKIA)_3$-NH_2 was significantly reduced [Blazyk, J., et al. (2001) *J. Biol. Chem. 276*, 27899−27906]. In this paper, we measured the lytic properties of these peptides, as well as several fluorescent analogues containing a single tryptophan residue, by monitoring permeability changes in large unilamellar vesicles with varying lipid compositions and in *Escherichia coli* cells. The binding of these peptides to lipid bilayers with defined compositions was compared using surface plasmon resonance, circular dichroism, and fluorescence spectroscopy. Surprisingly large differences were observed in membrane binding properties, particularly in the case of KIGAKIKWGAKIKIGAKI-NH_2. Since all of these peptides possess the same charge and very similar mean hydrophobicities, the binding data cannot be explained merely in terms of electrostatic and/or hydrophobic interactions. In light of their equivalent antimicrobial and hemolytic potencies, some of these peptides may employ mechanisms beyond simply increasing plasma membrane permeability to exert their lethal effects.

Most animals and plants use at least some antimicrobial cationic peptides as part of their defensive arsenal in combating infection by microorganisms. A wide variety of such peptides has been discovered over the past 20 years. In recent years, the dramatic rise in the resistance of virulent microorganisms to antibiotics currently in use has heightened interest in new antimicrobial agents. A great deal of effort has focused on how antimicrobial peptides function at the molecular level and whether the native peptides or their derivatives may be useful in fighting bacterial infection (*1*−*4*).

Naturally occurring cationic antimicrobial peptides can be divided into three main structural classes. Most linear peptides have the potential to adopt an amphipathic α-helical conformation. These peptides possess little or no structure in solution. When the peptides bind to membranes or lipid bilayers via electrostatic interactions, however, the formation of an amphipathic α-helix is believed to be a critical step in antimicrobial activity. Peptide-induced permeabilization of the plasma membrane is thought to result from either the formation of discrete pores (*5*, *6*) or a detergent-like effect (*7*). Examples of this class of antimicrobial peptides include insect cecropins, frog magainins, and human cathelicidins (*2*). A second structural class, including mammalian defensins (*8*) and protegrins (*9*), contains peptides with several intramolecular disulfide bonds that stabilize a conformation containing amphipathic β-sheets. These peptides also exert their antimicrobial effects primarily through membrane disruption. The third class includes extended peptides that are rich in one or two amino acids, such as indolicidin (*10*).

A large array of derivatives based upon these structural models has been synthesized and studied in an attempt to increase the potency and selectivity of the native antimicrobial peptides (*1*, *2*). For instance, it is possible to vary the length, charge, overall hydrophobicity, and amphipathic character of these peptides. In many cases, however, enhancing the antimicrobial potency is accompanied by a concomitant reduction in selectivity between bacterial and mammalian cells (as judged by hemolytic activity). It is apparent that a delicate balance exists between selective antimicrobial peptides and generally cytotoxic peptides such as melittin. The question of selectivity assumes great importance if a sufficiently high therapeutic index necessary for clinical use in animals is desired. Since the presumed initial target of these

† Supported by NIH Grant AI47165 (J.B.).

* To whom correspondence should be addressed. Telephone: (740) 593-1742. Fax: (740) 593-2320. E-mail: blazyk@ohiou.edu.

‡ Department of Chemistry and Biochemistry, College of Arts and Sciences, Ohio University.

§ Monash University.

|| College of Osteopathic Medicine, Ohio University.

⊥ Molecular and Cellular Biology Program, College of Arts and Sciences, Ohio University.

10.1021/bi034338s CCC: $25.00
Published on Web 07/18/2003

peptides is the bacterial plasma membrane surface and not specific receptors, antimicrobial peptides with enhanced binding properties for lipids on the surface of bacterial versus mammalian cells might help to enhance both activity and selectivity.

Recently, we tested a new design in which the amino acid sequence of a linear cationic peptide had the potential to form an amphipathic β-sheet instead of an α-helix (*11*). Our model β-sheet peptide, KIGAKI,[1] possessed antimicrobial activity equivalent to that of an analogous peptide, KIAGKIA, that has amphipathic α-helical properties but the same net charge and overall hydrophobicity. KIGAKI was much less potent at inducing leakage in LUV composed of POPC or POPC/POPG mixtures than KIAGKIA; however, in POPE/POPG LUV, the lytic activity of KIGAKI was enhanced while that of KIAGKIA was significantly reduced. While both of these peptides exhibited no secondary structure in solution, the expected conformations (i.e., β-sheet for KIGAKI and α-helix for KIAGKIA) were observed by CD and FTIR spectroscopy in the presence of anionic lipids. It should be noted that the structural properties of KIGAKI are significantly different from those of other β-sheet antimicrobial peptides such as defensins and tachyplesins. The latter peptides contain inherent structure resulting from the constraint of intramolecular disulfide bonds. The β-sheet structure observed in KIGAKI is induced by its interaction with the lipid bilayers. In fact, KIGAKI adopts α-helical structure in a 50% TFE/water mixture, so the association with the membrane surface is mandatory for β-sheet formation.

A common feature of these interactions is the induction of amphipathic secondary structure following electrostatic binding of the peptides to the lipid surface. Since selective binding to different phospholipids is central to the design of antimicrobial peptides that can discriminate between bacterial and mammalian cells, the affinity of the peptide for the membrane surface is a critical factor in the lytic process, but is not commonly measured and reported. We have utilized a new and sensitive method based on surface plasmon resonance (SPR), which allows the real-time measurement of the level of peptide binding to phospholipid membranes (*12*). This technique, which does not require the presence of labels or chromophores, is used in this work to assess dynamic peptide−lipid association and dissociation as a function of peptide concentration.

In our previous work (*11*), we made analogues of KIGAKI and KIAGKIA containing a single tryptophan residue at position 8 (W_8-KIGAKI) and position 9 (W_9-KIAGKIA), respectively, in each case replacing an isoleucine. Since the antimicrobial activity of the tryptophan-containing peptides was indistinguishable from that of the parent compounds, we used tryptophan fluorescence to assess the interaction of the peptides with lipid vesicles. Similar substitutions have been used previously for other antimicrobial peptides such as magainin 2 (*5*) and nisin (*13*). We also made two additional KIGAKI analogues with tryptophan at position 2 and at position 18 to determine whether the position of tryptophan may affect the behavior of the peptide. Previous studies showed that the addition of an octanoyl group can increase the antimicrobial potency of amphipathic α-helical peptides (*1*). Therefore, we tested an octanoylated analogue of W_8-KIGAKI to measure the effects on activity and binding. In this paper, we compare the structural and functional properties of the parent peptides with these tryptophan-containing analogues. Despite their nearly equipotent antimicrobial activity, striking differences in lipid binding and lytic activity were observed not only between the α-helical and β-sheet peptides but also among the β-sheet tryptophan analogues. These results suggest that a common mechanism for microbicidal activity involving only induction of plasma membrane leakage may be insufficient in explaining the action of these peptides.

MATERIALS AND METHODS

Materials. All peptides were synthesized using Fmoc chemistry by ResGen (Huntsville, AL). The crude peptides were purified by reverse-phase HPLC. Purity was checked by reverse-phase HPLC and electrospray mass spectrometry. POPC, POPE, and POPG were used as supplied from Avanti Polar Lipids, Inc. (Alabaster, AL). Calcein, CHAPS, TFE, and buffer materials were from Sigma Chemical Co. (St. Louis, MO). The phosphorus content in lipid stock solutions was determined by a spectrophotometric analysis (*14*).

Antimicrobial and Hemolytic Assays. Antimicrobial susceptibility testing against *Staphylococcus aureus* (ATCC 29213), *Escherichia coli* (ATCC 25922), and *Pseudomonas aeruginosa* (ATCC 27853) was performed using a modification of the National Committee for Clinical Laboratory Standards microdilution broth assay (*11*). Mueller-Hinton broth (BBL) was used for diluting the peptide stock solution and for diluting the bacterial inoculum. The inoculum was prepared from mid-logarithmic-phase cultures. Microtiter plate wells received aliquots of 100 μL each of the inoculum and peptide dilution. The final concentration of the peptide solution ranged from 0.5 to 64 μg/mL in 2-fold dilutions. The final concentration of bacteria in the wells was 5×10^5 cfu/mL. Peptides were tested in duplicate. In addition to the test peptide, three standard peptides and a nontreated growth control were included to validate the assay. The microtiter plates were incubated overnight at 37 °C, and the absorbance was measured at 600 nm. The MIC is defined as the lowest concentration of the peptide that completely inhibits growth of the organism.

The kinetics of bactericidal activity were measured as follows. Bacteria were incubated to midlogarithmic phase and diluted with medium to 10^6 cfu/mL. Peptide was added at a concentration of 30 μg/mL to initiate the experiment. At time intervals of 0, 5, 10, 20, 30, 60, 120, and 180 min, a 100 μL aliquot was removed and diluted 10^2-10^4-fold with

[1] Abbreviations: CD, circular dichroism; cfu, colony-forming units; CHAPS, 3-[(3-cholamidopropyl)dimethylammonio]-1-propanesulfonate; HEPES, 4-(2-hydroxyethyl)piperazine-1-ethanesulfonic acid; KIAGKIA, $(KIAGKIA)_3$-NH_2; KIGAKI, $(KIGAKI)_3$-NH_2; L/P, lipid-to-peptide; LUV, large unilamellar vesicles; μ_H, hydrophobic moment; MIC, minimum inhibitory concentration; Oct-W_8-KIGAKI, CH_3-$(CH_2)_6$-(C═O)-KIGAKIKWGAKIKIGAKI-NH_2; ONPG, *o*-nitrophenyl β-D-galactopyranoside; PC, phosphatidylcholine; PE, phosphatidylethanolamine; PG, phosphatidylglycerol; POPC, 1-palmitoyl-2-oleoylphosphatidylcholine; POPE, 1-palmitoyl-2-oleoylphosphatidylethanolamine; POPG, 1-palmitoyl-2-oleoylphosphatidylglycerol; SPR, surface plasmon resonance; SUV, small unilamellar vesicles; TFE, trifluoroethanol; W_9-KIAGKIA, KIAGKIAKWAGKIAKIAGKIA-NH_2; W_2-KIGAKI, KWGAKIKIGAKIKIGAKI-NH_2; W_8-KIGAKI, KIGAKIKWGAKIKIGAKI-NH_2; W_{18}-KIGAKI, KIGAKIKIGAKIKIGAKW-NH_2.

medium containing 0.5 M NaCl. A 100 μL aliquot of this mixture was applied to a Mueller-Hinton agar plate. After overnight growth at 37 °C, the colony-forming units were counted. The kinetic determination of bactericidal activity was recorded as the number of surviving colonies versus incubation time in the presence of peptide.

Hemolysis at a peptide concentration of 100 or 500 μg/mL was assessed using a 5% suspension of freshly drawn human erythrocytes, which had been washed twice in phosphate-buffered saline (*11*). After incubation at 37 °C for 30 min, the suspension was centrifuged at 10000*g* for 10 min and the absorbance at 400 nm was measured. Complete hemolysis was realized by adding 0.2% Triton X-100 in place of the peptide.

CD Spectroscopy. CD spectra were measured in a 1 mm quartz cuvette using a Jasco J-715 spectropolarimeter. Spectra were recorded from 250 to 190 nm at a sensitivity of 100 mdeg, a resolution of 0.5 nm, a response of 8 s, a bandwidth of 1.0 nm, and a scan speed of 50 nm/min, with a single accumulation. The buffer contained 5 mM potassium phosphate (pH 7.0). The peptide concentration was 20 μM. LUV were prepared from aqueous dispersions of phospholipids at a concentration of ~1 mg/mL in phosphate buffer. Following five freeze−thaw cycles, the mixture was extruded 10 times through a 0.1 μm pore polycarbonate membrane in an Avanti mini-extruder apparatus, resulting in ~100 nm diameter LUV.

Peptide-Induced Leakage of ONPG into E. coli ML-35 Cells. Diffusion of extracellular ONPG into the cytoplasm of *E. coli* ML-35 cells was monitored according to the method of Skerlavaj et al. (*15*). *E. coli* ML-35 cells constitutively express cytoplasmic β-galactosidase and are lactose permease deficient, thus preventing the uptake of ONPG. The extent of peptide-induced permeabilization of the plasma membrane is measured by the rate of production of *o*-nitrophenol, which absorbs strongly at 405 nm, following release of galactose via β-galactosidase. A 100 μL aliquot of logarithmic-phase *E. coli* ML-35 cells (10^8 cfu/mL) was added to 700 μL of 10 mM sodium phosphate, 100 mM NaCl, and 1.5 mM ONPG (pH 7.5) in a 37 °C preheated cuvette. A 200 μL aliquot containing the desired concentration of peptide was added at time zero. An equivalent volume of 0.5% TFA replaced the peptide solution in the negative control. The rate of *o*-nitrophenol production was monitored at 405 nm for 15 min. Complete permeabilization (100% control) was assessed using sonicated bacteria. None of the peptides had any direct effect upon β-galactosidase activity. In all cases, the reaction rate was linear over the 15 min time course. The percent maximal rate of ONPG cleavage was calculated from the ratio of the peptide-induced reaction rate to that of the 100% control.

Peptide-Induced Leakage from Calcein-Loaded LUV. The ability of the peptides to release calcein (M_r = 623) from LUV with varying lipid compositions was compared. LUV were prepared as described above, except that the buffer consisted of 50 mM HEPES, 100 mM NaCl, 0.3 mM EDTA, and 80 mM calcein (pH 7.4). Calcein-loaded vesicles were separated from free calcein by size-exclusion chromatography using a Sephadex G-50 column and calcein-free buffer. Calcein leakage was monitored using a Varian Cary (Walnut Creek, CA) Eclipse spectrofluorometer by measuring the time-dependent increase in the fluorescence of calcein (excitation at 490 nm, emission at 520 nm). Assays were performed by assessing eight wells simultaneously in a 96-well plate. A 180 μL aliquot of the LUV suspension was added to each well using a multichannel pipet, followed by a 20 μL aliquot of peptide solutions at varying concentrations to give the desired lipid-to-peptide (L/P) ratio of 2−256. The final concentration of lipid in the assay was 10 μM. Peptide was omitted from a negative control. Complete leakage was realized by the addition of 20 μL of 10% Triton X-100 in place of peptide. Each value represents at least six separate measurements using at least two different LUV preparations. We determined that the percentage of calcein leakage at 3 min following the addition of the peptide represents at least 90% of the maximal leakage. For all the peptides that were tested, maximal leakage was observed after 10−15 min.

Surface Plasmon Resonance Measurements of Peptide Binding to LUV. Biosensor experiments were carried out with a BIACORE X analytical system using the Pioneer L1 sensor chip (Biacore AB, Uppsala, Sweden) at an operation temperature of 25 °C. The Pioneer L1 sensor chip is composed of alkyl chains covalently linked to a dextran-coated gold surface. The running buffer was 0.02 M sodium phosphate (pH 6.8); the washing solution was 40 mM CHAPS, and the regeneration solution was 10 mM sodium hydroxide. All solutions were freshly prepared, degassed, and filtered through a 0.22 μm filter. SUV (~50 nm diameter) with a 4/1 POPE/POPG or 4/1 POPC/POPG ratio were prepared in 0.02 M phosphate buffer by sonication and extrusion as previously described (*12*).

The BIACORE X instrument was cleaned extensively and left running overnight using Milli-Q water to remove trace amounts of detergent. The surface of the L1 sensor chip was cleaned by an injection of the nonionic detergent 40 mM CHAPS (25 μL) at a flow rate of 5 μL/min. SUV (80 μL, 0.5 mM) were applied to the sensor chip surface at a low flow rate, and the liposomes were captured on the surface of the sensor chip by the lipophilic compounds and provided a supported lipid bilayer. To remove any multilamellar structures from the lipid surface, sodium hydroxide (30 μL, 10 mM) was injected at flow rate of 50 μL/min, which resulted in a stable baseline corresponding to the immobilized liposome bilayer membrane.

Peptide solutions were prepared by dissolving each peptide in 0.02 M phosphate buffer (pH 6.8) from 5 to 40 μM. The solutions (80 μL, 980 s) were injected over the lipid surface at a flow rate of 5 μL/min. The peptide solution was replaced with 0.02 M phosphate buffer (pH 6.8), and the peptide−liposome complex was allowed to dissociate for 1200 s. Since the peptide−lipid interactions are very hydrophobic, the regeneration of the liposome surface was not possible. The immobilized liposomes were therefore completely removed with an injection of 40 mM CHAPS, and each peptide injection was performed on a freshly prepared liposome surface. All binding experiments were carried out at 25 °C. The affinity of the peptide−lipid binding event was estimated from analysis of a series of response curves. In each case, the resultant sensorgrams were collected at seven different peptide concentrations injected over each lipid surface for each peptide. The peptide concentrations ranged from 2 to 50 μM for binding experiments on both liposome surfaces.

In the case of KIAGKIA, the complete dissociation of the peptide from the immobilized liposome surface took ap-

proximately 1−1.5 h, depending on the peptide and the type of liposome used in the binding study, after which the immobilized liposome surface became reusable for further peptide injections. In contrast, none of the sensorgrams for KIGAKI returned to the lipid baseline following dissociation, indicating that a proportion of the peptide remained bound to the liposomes. As a result, the immobilized liposome surface was replaced with a new surface before each new peptide injection.

The sensorgrams for each peptide−lipid interaction were analyzed by curve fitting using numerical integration analysis. The data were fitted globally by simultaneously fitting the peptide sensorgrams obtained in duplicate at seven different concentrations ranging from 2 to 50 μM. Since a poor fit was obtained with the simple 1/1 binding model, the two-state reaction model was applied to the sensorgrams to determine the association and dissociation rate constants. This model describes two reaction steps, which in terms of peptide−lipid interaction may correspond to

$$\mathrm{P} + \mathrm{L} \Leftrightarrow \mathrm{PL} \Leftrightarrow \mathrm{PL}^* \quad (1)$$

where peptide (P) binds to lipids (L) to give the complex PL as a result of initial electrostatic binding. PL subsequently changes to PL*, which represents the penetration of the peptide into the hydrophobic region of the lipid bilayer and formation of amphipathic secondary structure. PL* cannot dissociate directly to P and L. The corresponding differential rate equations for this reaction model are represented by

$$dR_1/dt = k_{a1}C_A(R_{max} - R_1 - R_2) - k_{d1}R_1 - k_{a2}R_1 + k_{d2}R_2 \quad (2)$$

$$dR_2/dt = k_{a2}R_1 - k_{d2}R_2 \quad (3)$$

Peptide Binding to LUV Measured by Tryptophan Fluorescence. Peptide interactions with LUV were assessed using a Varian Cary Eclipse spectrofluorometer equipped with a manual polarizer accessory, according to the method developed by Ladokhin et al. (*16*). Fluorescence emission spectra were collected from 290 to 500 nm at 1 nm increments using an excitation wavelength of 280 nm at a signal-to-noise ratio of 500 using a 2 mm × 10 mm quartz cuvette at 25 °C. Excitation and emission slit widths were 10 and 5 nm, respectively. LUV were prepared as described above using a buffer containing 50 mM HEPES, 100 mM NaCl, and 0.3 mM EDTA (pH 7.4). Lipid-to-peptide ratios of 1, 5, 10, 15, 20, and 50 were measured at a constant peptide concentration of 10 μM.

All spectra were collected using emission and excitation polarizers oriented at 90° and 0° relative to the vertical, respectively. Peptide interactions with LUV were assessed by the tryptophan emission intensity at 330 nm. Measured intensity values at 330 nm were corrected for light scattering effects of LUV at each lipid concentration using the ratio of intensities at 330 nm of 10 μM tryptophan in the absence and presence of LUV as shown in the following equation:

$$I_{corrected} = I_{measured}\frac{I_{Trp+buffer}}{I_{Trp+LUV}} \quad (4)$$

These corrected intensity values then were used to estimate the fluorescence increase upon complete binding (I_∞) and the mole fraction partition coefficient (K_x) using the following equation:

$$I([L]) = 1 + (I_\infty - 1)\frac{K_x[L]}{[W] + K_x[L]} \quad (5)$$

where [L] is the lipid concentration, I([L]) is the corrected intensity at each lipid concentration, and [W] equals 55.3 M, the molar concentration of water (*16*). Values for I_∞ and K_x were determined by fitting the data to eq 5 using GraphPad Prism version 3.02 for Windows (GraphPad Software, San Diego, CA).

Table 1: Amino Acid Sequences of Antimicrobial Peptides

	1 5 10 15 20
KIAGKIA	K I A G K I A K I A G K I A K I A G K I A – NH_2
W_9-KIAGKIA	K I A G K I A K W A G K I A K I A G K I A – NH_2
KIGAKI	K I G A K I K I G A K I K I G A K I – NH_2
W_2-KIGAKI	K W G A K I K I G A K I K I G A K I – NH_2
W_8-KIGAKI	K I G A K I K W G A K I K I G A K I – NH_2
W_{18}-KIGAKI	K I G A K I K I G A K I K I G A K W – NH_2

Table 2: Antimicrobial Activities of Model Peptides

	minimum inhibitory concentration (μg/mL)[b]			
peptide[a]	*E. coli* ML-35	*E. coli* ATCC 25922	*S. aureus* ATCC 29213	*P. aeruginosa* ATCC 27853
KIAGKIA	2	8	16	4
W_9-KIAGKIA	2	8	16	8
KIGAKI	2	8	8	8
W_2-KIGAKI	4	4	4	4
W_8-KIGAKI	2	8	8	8
Oct-W_8-KIGAKI	4	8	4	8
W_{18}-KIGAKI	4	8	16	8

[a] See Table 1 for peptide sequences. [b] For minimum inhibitory concentrations, differences of a factor of greater than 2 are considered significant.

RESULTS

Comparison of Antimicrobial and Hemolytic Activities of the Peptides. The antimicrobial activities of KIGAKI, W_8-KIGAKI, W_2-KIGAKI, W_{18}-KIGAKI, Oct-W_8-KIGAKI, KIAGKIA, and W_9-KIAGKIA are listed in Table 2. No significant differences in potency were observed among these peptides for either Gram-positive or Gram-negative microorganisms, except that W_{18}-KIGAKI is less active against all the test bacteria. The *E. coli* ML-35 strain was the most susceptible of the four bacterial strains that were tested. At 500 μg/mL, all of the peptides that were tested exhibited little hemolytic activity (<10%) except for Oct-W_{18}-KIGAKI (40%). Even at 100 μg/mL, Oct-W_8-KIGAKI exhibited higher hemolytic activity than the other peptides at 500 μg/mL.

Peptide-Induced Leakage from Calcein-Loaded LUV. We previously compared the lytic activity of KIGAKI and KIAGKIA with LUV with varying lipid compositions (*11*). KIAGKIA was more potent than KIGAKI at inducing calcein release from LUV composed of POPC, POPG, or mixtures of POPC and POPG. In contrast, KIGAKI was more effective at promoting leakage from POPE/POPG LUV. Since the tryptophan analogues of these peptides were indistinguishable

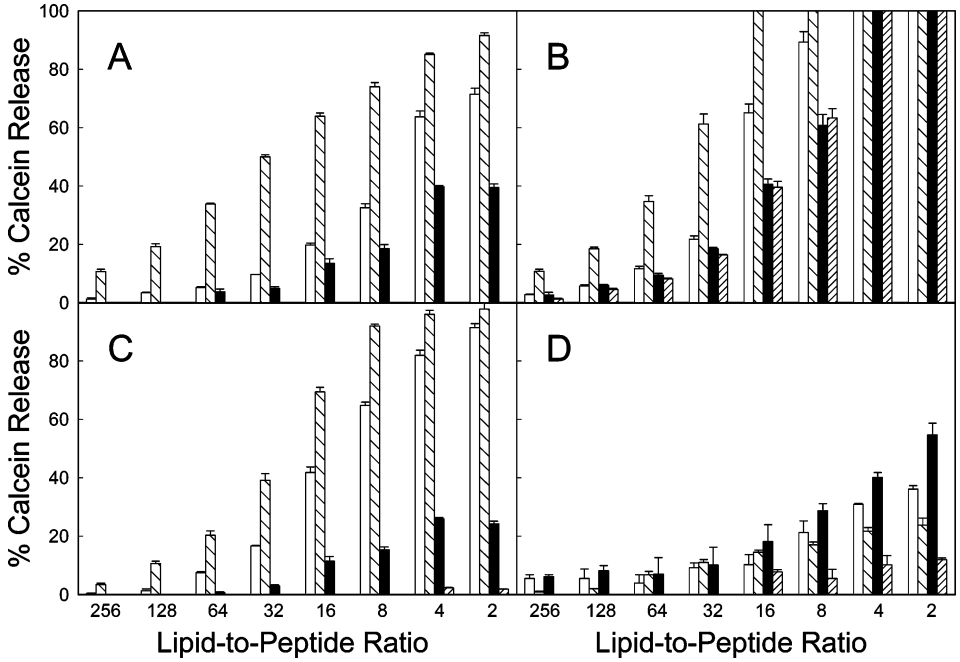

FIGURE 1: Percent release of calcein from LUV 3 min after the addition of KIAGKIA (white bars), W_9-KIAGKIA (coarsely hatched bars), KIGAKI (black bars), or W_8-KIGAKI (finely hatched bars): (A) POPC, (B) POPG, (C) 4/1 POPC/POPG, and (D) 4/1 POPE/POPG LUV.

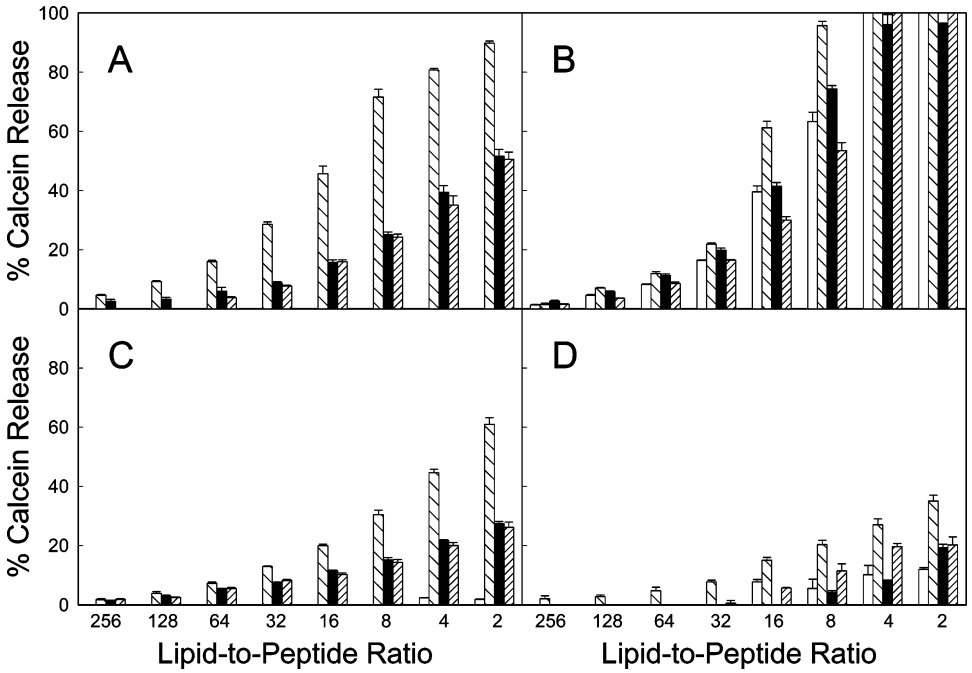

FIGURE 2: Percent release of calcein from LUV 3 min after the addition of W_8-KIGAKI (white bars), Oct-W_8-KIGAKI (coarsely hatched bars), W_2-KIGAKI (black bars), or W_{18}-KIGAKI (finely hatched bars): (A) POPC, (B) POPG, (C) 4/1 POPC/POPG, and (D) 4/1 POPE/POPG LUV.

in terms of antimicrobial activity from the parent peptides, we expected similar lytic potencies with LUV. A comparison of the lytic activity of KIAGKIA, W_9-KIAGKIA, KIGAKI, and W_8-KIGAKI in either POPC, POPG, 4/1 POPC/POPG, or 4/1 POPE/POPG LUV at L/P ratios ranging from 256 to 2 is shown in Figure 1. The general trends observed previously are confirmed here; however, several notable differences exist between the peptide pairs with and without tryptophan. W_9-KIAGKIA is slightly better at inducing calcein release from POPC LUV and 4/1 POPC/POPG LUV than KIAGKIA. In contrast, W_8-KIGAKI is much less active than KIGAKI in these lipid systems. A similar difference between W_8-KIGAKI and KIGAKI is observed in 4/1 POPE/POPG LUV, especially at low L/P ratios. The most striking observation is the weak lytic potency of W_8-KIGAKI in all lipid systems except POPG.

A comparison of the lytic activities of W_8-KIGAKI, Oct-W_8-KIGAKI, W_2-KIGAKI, and W_{18}-KIGAKI in either POPC, POPG, 4/1 POPC/POPG, or 4/1 POPE/POPG LUV at L/P ratios ranging from 256 to 2 is shown in Figure 2. W_8-KIGAKI was significantly less active than W_2-KIGAKI and W_{18}-KIGAKI in POPC LUV and 4/1 POPC/POPG LUV. Oct-W_8-KIGAKI induced more leakage in all LUV that were tested, but especially in POPC and 4/1 POPC/POPG LUV.

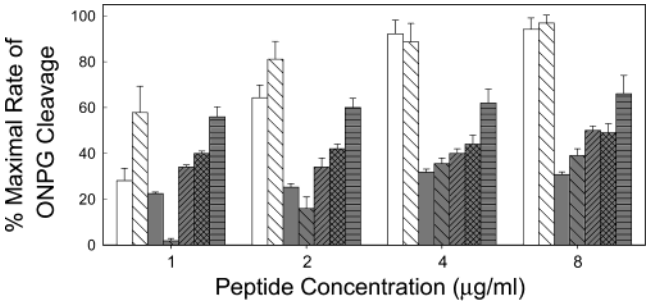

FIGURE 3: Concentration dependence of peptide-induced leakage of extracellular ONPG into the cytoplasm of *E. coli* ML-35 cells following the addition of KIAGKIA (white bars), W_9-KIAGKIA (coarsely hatched white bars), KIGAKI (gray bars), W_8-KIGAKI (coarsely hatched gray bars), Oct-W_8-KIGAKI (finely hatched gray bars), W_2-KIGAKI (cross-hatched gray bars), and W_{18}-KIGAKI (horizontally hatched gray bars).

Peptide-Induced Permeability in the Plasma Membrane of E. coli ML-35. All of the peptides tested here could inhibit the growth of *E. coli* ML-35 at a concentration of 2−4 μg/mL. In the absence of peptide, exogenous ONPG cannot be cleaved by cytoplasmic β-galactosidase. Figure 3 shows the ability of the peptides to enhance ONPG cleavage in comparison to a sonicated bacterial control. It is clear that KIAGKIA and W_9-KIAGKIA were more effective than KIGAKI and its tryptophan analogues at inducing ONPG permeability, even at peptide concentrations greater than the MIC values. At 1 μg/mL, W_9-KIAGKIA was more active than KIAGKIA, while KIGAKI was substantially more potent than W_8-KIGAKI, which correlates with the calcein leakage results. At ≥ 2 μg/mL, no significant differences were observed between these peptide pairs. Of the tryptophan-containing analogues of KIGAKI, W_8-KIGAKI was the least potent, especially at lower concentrations, while W_{18}-KIGAKI was the most potent; however, even W_{18}-KIGAKI was less active than either KIAGKIA or W_9-KIAGKIA at concentrations greater than the MIC values.

CD Spectroscopy of Peptide/Lipid Mixtures. CD spectra of KIAGKIA, W_9-KIAGKIA, KIGAKI, and W_8-KIGAKI in the presence of LUV with varying lipid compositions are shown in Figure 4. The L/P ratio was constant at 50. With neutral POPC LUV (panel A), the spectra were characteristic of random structure (with a minimum below 200 nm) and were indistinguishable from spectra of the peptides in buffer (data not shown). In the presence of anionic POPG LUV (panel B), however, the spectra of KIAGKIA and W_9-KIAGKIA exhibited a large maximum near 190−195 nm and minima near 208 and 222 nm, characteristic of α-helical structure. In contrast, both KIGAKI and W_8-KIGAKI exhibited a maximum near 200 nm and a single minimum just below 220 nm, indicating β-sheet structure (*17*). A comparison of the CD spectra in 4/1 POPC/POPG (panel C) and 4/1 POPE/POPG (panel D) LUV shows clear differences in lipid selectivity among these peptides. Although the signal was substantially weaker than with POPG LUV, both KIAGKIA and W_9-KIAGKIA exhibited an α-helical conformation in the presence of PC-containing LUV, but this structure was almost completely lost in the presence of PE-containing LUV. In contrast, KIGAKI and W_8-KIGAKI showed little structure with PC-containing LUV, while KIGAKI clearly adopted some β-sheet structure with PE-containing LUV.

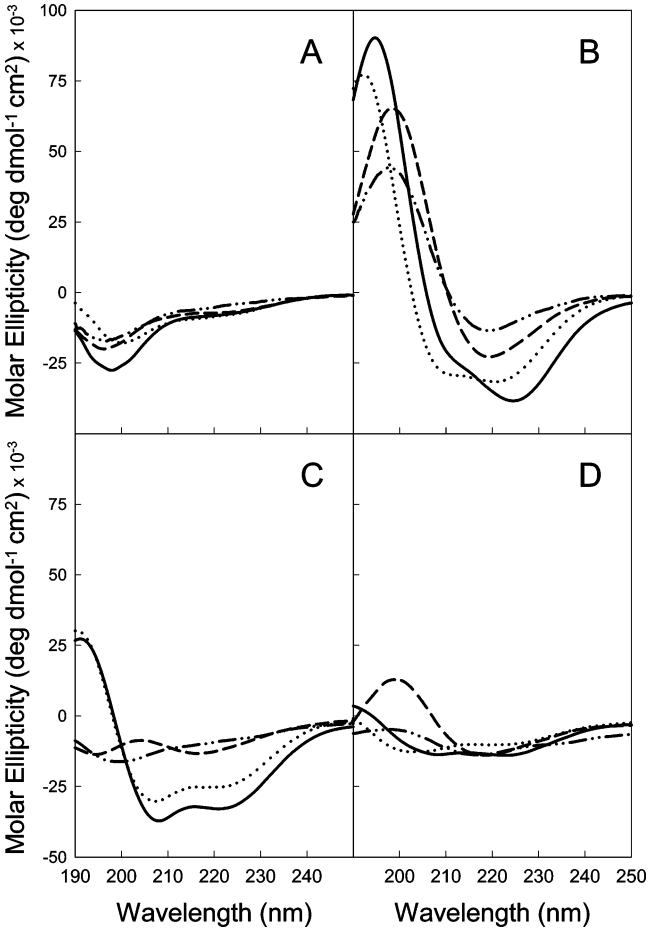

FIGURE 4: CD spectra of KIAGKIA (—), W_9-KIAGKIA (···), KIGAKI (− − −), and W_8-KIGAKI (−··−) in the presence of (A) POPC LUV, (B) POPG LUV, (C) 4/1 POPC/POPG LUV, and (D) 4/1 POPE/POPG LUV at a lipid-to-peptide ratio of 50.

The CD spectra of W_8-KIGAKI, Oct-W_8-KIGAKI, W_2-KIGAKI, and W_{18}-KIGAKI in the presence of LUV with varying lipid compositions are compared in Figure 5. All of these peptides exhibited random structure with POPC LUV (panel A) and a β-sheet conformation with POPG LUV (panel B). No significant differences were observed among the four peptides. In the presence of 4/1 POPC/POPG LUV (panel C), none of the peptides showed defined structure. In the presence of 4/1 POPE/POPG LUV (panel D), only Oct-W_8-KIGAKI exhibited some β-sheet structure, although much less than with POPG LUV. Thus, the presence of tryptophan at either position 2, 8, or 18 in KIGAKI limited the ability of the peptides to adopt β-sheet structure in comparison to the parent compound with both POPG LUV and 4/1 POPE/POPG LUV.

Surface Plasmon Resonance Measurements. KIAGKIA and KIGAKI appear to interact quite differently with LUV containing POPG and either POPC or POPE. To determine whether the CD results arise from differences in the amount of peptide binding to LUV or differences in the conformation of the bound peptide, we employed SPR spectroscopy to directly assess the binding for KIAGKIA and KIGAKI. SPR sensorgrams for binding to 4/1 POPC/POPG and 4/1 POPE/POPG at a peptide concentration of 50 μM are shown in Figure 6. Striking differences were observed between KIAGKIA, which exhibited a distinct association and dissociation, and KIGAKI, which had a very slow association on

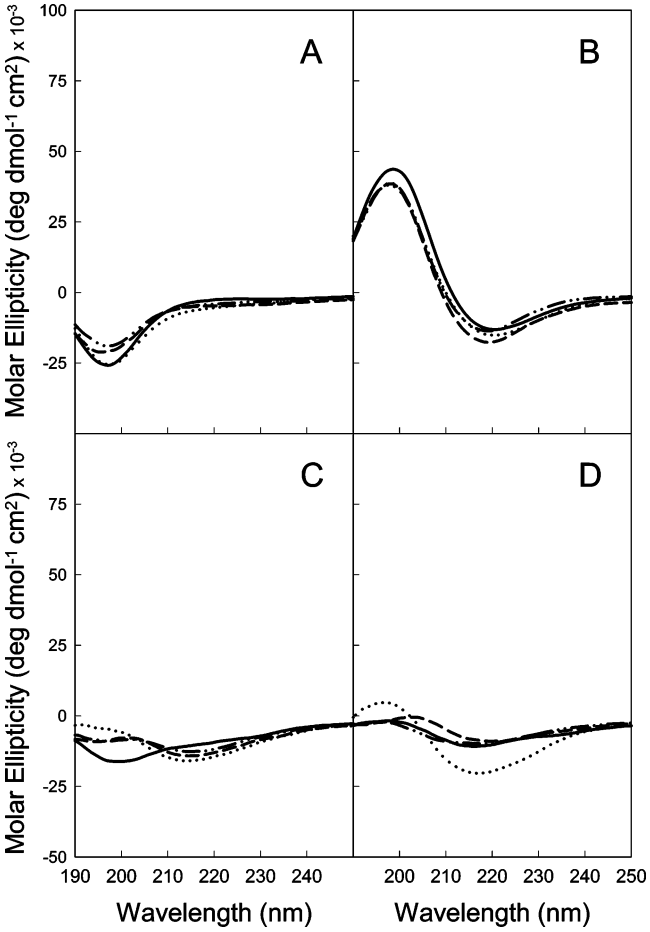

FIGURE 5: CD spectra of W_8-KIGAKI (—), Oct-W_8-KIGAKI (•••), W_2-KIGAKI (– – –), and W_{18}-KIGAKI (—••—) in the presence of (A) POPC LUV, (B) POPG LUV, (C) 4/1 POPC/POPG LUV, and (D) 4/1 POPE/POPG LUV at a lipid-to-peptide ratio of 50.

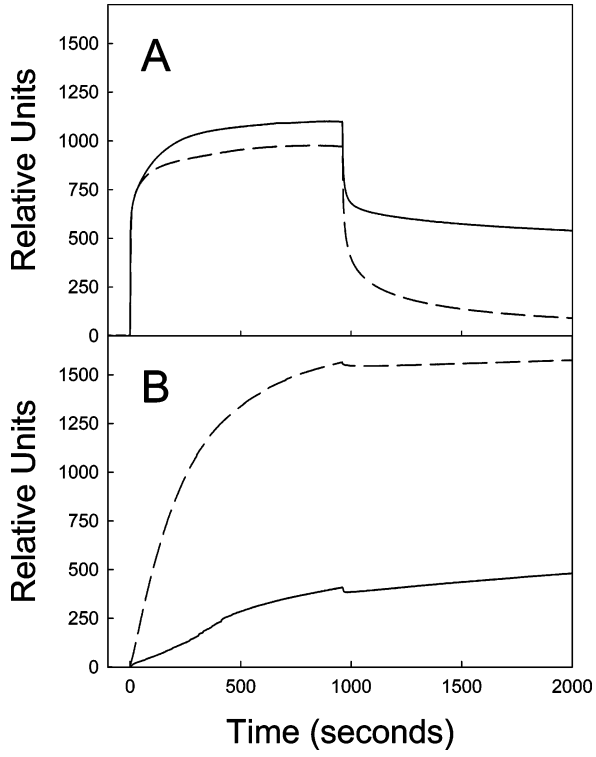

FIGURE 6: Surface plasmon resonance sensorgrams representing the association−dissociation curves for (A) KIAGKIA and (B) KIGAKI interacting with 4/1 POPC/POPG LUV (—) or 4/1 POPE/POPG LUV (– – –) on an L1 sensor chip. Association was assessed with a peptide solution [50 μM in 0.02 M phosphate buffer (pH 6.8)] at a flow rate of 5 μL/min for 980 s. Dissociation was assessed using the same buffer (without peptide) and flow rate for 1200 s.

both types of liposome surfaces. Furthermore, KIGAKI failed to dissociate from 4/1 POPC/POPG LUV (data not shown) at any concentration, thus preventing the calculation of kinetic values for this system. KIGAKI also exhibited a very slow rate of dissociation from 4/1 POPE/POPG LUV (data not shown) at lower peptide concentrations and no dissociation at higher concentrations. Consequently, no association constants could be calculated for 4/1 POPC/POPG LUV. Only peptide sensorgrams obtained at low peptide concentrations (5−20 μM) were used to calculate the association constants for KIGAKI with 4/1 POPE/POPG LUV.

The association constants, determined by the two-state reaction model (Table 3), show that KIAGKIA had a higher binding affinity for 4/1 POPC/POPG than for 4/1 POPE/POPG LUV. In contrast, KIGAKI displayed a higher binding affinity for 4/1 POPE/POPG LUV.

Fluorescence Emission in Peptide/Lipid Mixtures of Tryptophan-Containing Analogues. Emission spectra of the tryptophan-containing peptides W_9-KIAGKIA, W_8-KIGAKI, Oct-W_8-KIGAKI, W_2-KIGAKI, and W_{18}-KIGAKI were monitored in the presence of LUV with varying lipid compositions at L/P ratios ranging from 1 to 50. In aqueous solution in the absence of lipids, the emission spectra for the peptides were nearly identical, with maxima near 355−356 nm. The influence of LUV upon fluorescence emission properties was assessed by measuring lipid concentration-dependent changes in intensity at 330 nm. Lipid−peptide association generally results in both a blue shift and an increase in intensity in the emission spectrum. Since the change in the emission maximum does not correlate linearly with the proportion of peptide bound, we used the method of Ladokhin et al. (*16*) as a linear estimate of the extent of peptide binding.

The change in tryptophan emission intensity at 330 nm (corrected for scattering effects as described in Materials and Methods) was monitored as a function of the L/P ratio. No changes were observed for any of these peptides in the presence of LUV containing only POPC. Figure 7 shows the results for these peptides in the presence of POPG, 4/1 POPC/POPG, and 4/1 POPE/POPG LUV. The largest increase in intensity was observed for W_9-KIAGKIA (panel A), with a more than 4-fold enhancement in the presence of POPG LUV. LUV with a 4/1 POPC/POPG ratio induced a much greater increase in intensity than 4/1 POPE/POPG LUV, indicating that W_9-KIAGKIA associates more strongly with PC-containing LUV. This is reflected in the values for I_∞ and K_x that were calculated from curve fitting results using eq 5 (Table 4).

For the four tryptophan-containing analogues of KIGAKI (panels B−E), the increase in intensity induced by POPG LUV was much smaller than that with W_9-KIAGKIA (see the values of I_∞ and K_x in Table 4) for the KIGAKI analogues. These peptides differed significantly in their associations with 4/1 POPC/POPG and 4/1 POPE/POPG LUV. Almost no increase in intensity at 330 nm was

Table 3: Association (k_{a1} and k_{a2}) and Dissociation (k_{d1} and k_{d2}) Rate Constants Determined by Numerical Integration Using the Two-State Reaction Model, and the Affinity Constant (K) Determined as (k_{a1}/k_{d1})(k_{a2}/k_{d2})

peptide	lipid type	k_{a1} (M^{-1} s^{-1})	k_{d1} (s^{-1})	k_{a2} (M^{-1} s^{-1})	k_{d2} (s^{-1})	K (M^{-1})
		Bilayer Study with the L1 Sensor Chip				
KIAGKIA	PC/PG	2505	423×10^{-4}	34×10^{-4}	5.5×10^{-4}	37×10^{-4}
	PE/PG	1580	293×10^{-4}	9×10^{-4}	17×10^{-4}	3×10^{-4}
KIGAKI	PC/PG	–	–	–	–	–
	PG/PG	332	39×10^{-4}	17×10^{-4}	2.7×10^{-4}	54×10^{-4}

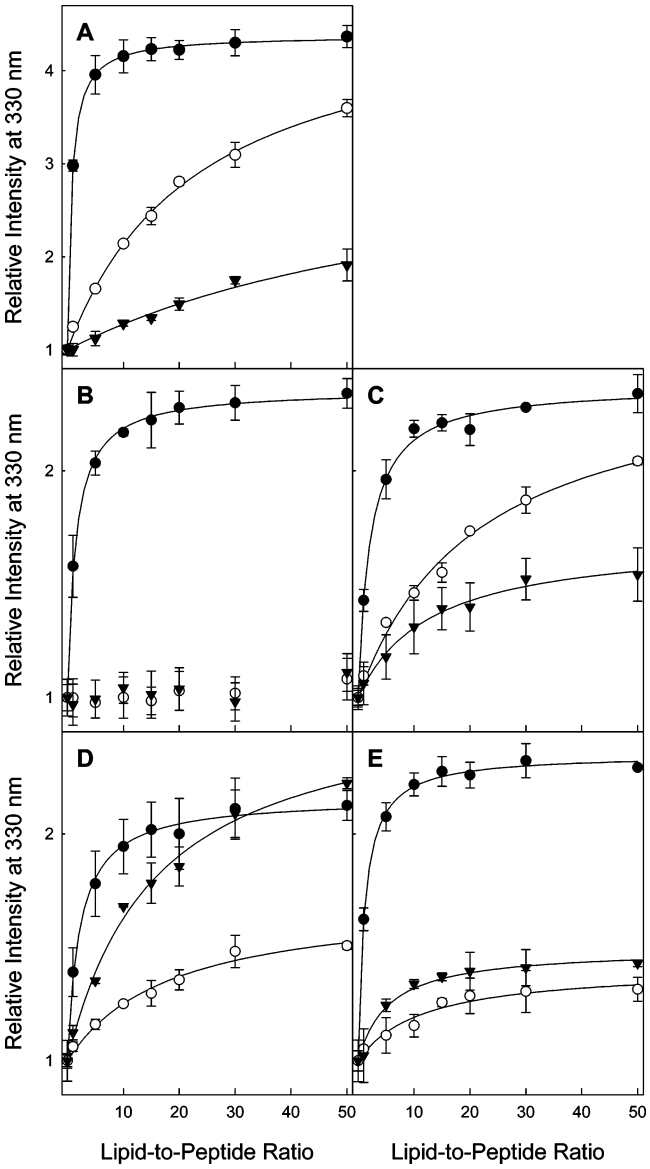

FIGURE 7: Relative intensity changes in the tryptophan emission at 330 nm as a function of lipid-to-peptide ratio for POPG LUV (●), 4/1 POPC/POPG LUV (○), and 4/1 POPE/POPG LUV (▼) for (A) W_9-KIAGKIA, (B) W_8-KIGAKI, (C) Oct-W_8-KIGAKI, (D) W_2-KIGAKI, and (E) W_{18}-KIGAKI. The solid lines represent the results of curve fitting using eq 5. The peptide concentration was held constant at 10 μM for all measurements. The intensities were corrected for scattering effects as described in Materials and Methods.

observed with either of these lipid systems for W_8-KIGAKI (panel B). The addition of an octanoyl group to the amino terminus of this peptide resulted in a much larger increase in intensity at an L/P ratio of 50 with 4/1 POPC/POPG LUV than with 4/1 POPE/POPG LUV (panel C), arising from a significantly higher value of I_∞, even though K_x was lower for the PC-containing LUV (Table 4). For W_2-KIGAKI (panel D), the increase in intensity at 330 nm was much greater for 4/1 POPE/POPG LUV than for 4/1 POPC/POPG LUV, and was comparable to that observed for POPG LUV at an L/P ratio of 50 (see the I_∞ values in Table 4). Finally, in the case of W_{18}-KIGAKI (panel E), the increase in intensity at 330 nm was more similar for the PC- and PE-containing LUV, although the K_x value measured with 4/1 POPE/POPG LUV was approximately twice that measured with 4/1 POPC/POPG LUV (Table 4).

Kinetics of Bactericidal Activity of the Tryptophan-Containing KIGAKI Analogues. While the lipid binding properties of W_8-KIGAKI are considerably different from those of analogues Oct-W_8-KIGAKI, W_2-KIGAKI, and W_{18}-KIGAKI, the MIC values of all of these peptides are nearly identical, reflecting the antimicrobial activity of the peptides after overnight incubation. To assess how quickly the peptides exert their antimicrobial activity, a time dependence study of bactericidal action was undertaken. Here, bacteria were exposed to a peptide for a defined time interval between 5 and 180 min. Aliquots were then diluted in high-salt medium, spread on plates, and grown overnight to determine the extent of viability. Figure 8 shows the number of surviving cells (colony-forming units per milliliter) as a function of incubation time for *S. aureus* (panel A), *E. coli* (panel B), and *P. aeruginosa* (panel C). For all of the peptides, the killing process is significantly slower for *S. aureus* (60−180 min) than for *E. coli* or *P. aeruginosa* (10−60 min). It is clear that the addition of an octanoyl group to W_8-KIGAKI increases the rate at which this peptide exerts its bactericidal effect on all three organisms. W_2-KIGAKI and W_{18}-KIGAKI are more rapid in their bactericidal action than W_8-KIGAKI, but not as fast as Oct-W_8-KIGAKI.

DISCUSSION

Recently, we showed that KIGAKI, a linear cationic peptide with the potential to form a highly amphipathic β-sheet, has high antimicrobial activity and low hemolytic activity and is more selective for the neutral phospholipid PE, found in many bacterial plasma membranes, than for PC, found in mammalian membranes (*11*). We compared the structural and functional properties of KIGAKI to those of KIAGKIA, a linear cationic peptide with a similar charge and hydrophobicity that can form an amphipathic α-helix. In that work, we employed the tryptophan-containing analogues W_8-KIGAKI and W_9-KIAGKIA, assuming that they would exhibit lytic and lipid binding properties similar to those of their parent peptides, KIGAKI and KIAGKIA, respectively, since the analogues possessed nearly identical antimicrobial and hemolytic activities (Table 2).

Upon further study, however, it became clear that the lytic activity of W_8-KIGAKI was much lower than that of KIGAKI (Figure 1). Only with POPG LUV did W_8-KIGAKI have a lytic potency comparable to that of KIGAKI. In LUV

Table 4: Peptide Binding to LUV As Assessed by Changes in the Tryptophan Emission Spectral Intensity at 330 nm[a]

	POPG LUV		4/1 POPC/POPG LUV		4/1 POPE/POPG LUV	
peptide	I_∞	K_x ($\times 10^{-3}$)	I_∞	K_x ($\times 10^{-3}$)	I_∞	K_x ($\times 10^{-3}$)
W_9-KIAGKIA	4.38 ± 0.01	7.8 ± 0.2	4.79 ± 0.16	0.24 ± 0.02	3.36 ± 0.53	0.07 ± 0.02
W_8-KIGAKI	2.34 ± 0.01	3.8 ± 0.2	–	–	–	–
Oct-W_8-KIGAKI	2.38 ± 0.02	2.6 ± 0.3	2.48 ± 0.10	0.26 ± 0.04	1.70 ± 0.04	0.44 ± 0.06
W_2-KIGAKI	2.16 ± 0.02	2.5 ± 0.3	1.71 ± 0.06	0.30 ± 0.06	2.61 ± 0.08	0.35 ± 0.04
W_{18}-KIGAKI	2.35 ± 0.01	4.7 ± 0.3	1.41 ± 0.04	0.48 ± 0.14	1.49 ± 0.03	1.1 ± 0.2

[a] The parameters I_∞ (fluorescence increase upon complete binding) and K_x (mole fraction partition coefficient) were calculated by fitting the experimental data to eq 5 (*16*).

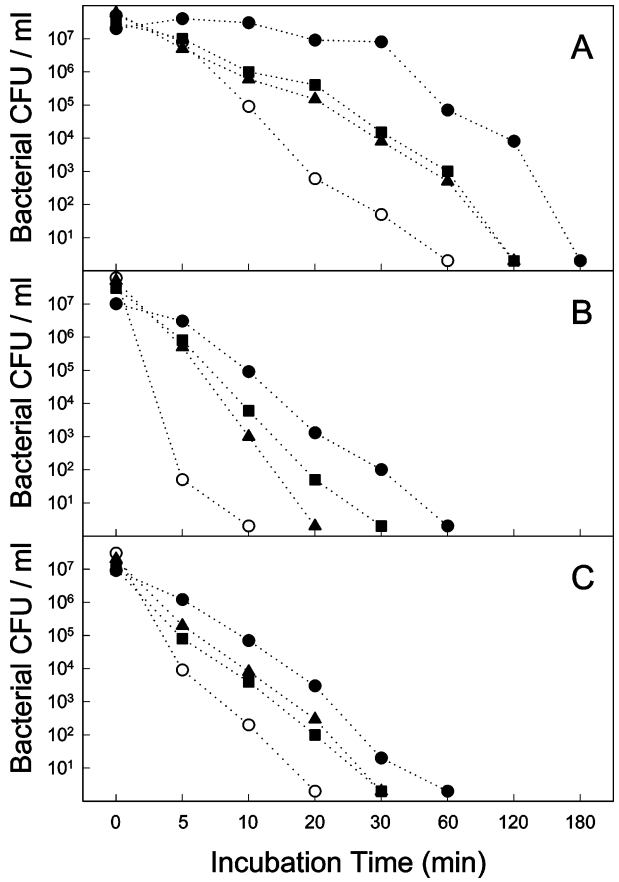

FIGURE 8: Kinetics of bactericidal action of W_8-KIGAKI (●), Oct-W_8-KIGAKI (○), W_2-KIGAKI (■), and W_{18}-KIGAKI (▲). The data are expressed as bacterial colony-forming units per milliliter, representing the number of viable bacteria per milliliter of culture medium, as a function of incubation time with peptide at a concentration of 30 μg/mL, for (A) *S. aureus*, (B) *E. coli*, and (C) *P. aeruginosa*.

containing neutral POPC or POPE as the major component, W_8-KIGAKI was not able to induce significant leakage even at very high peptide concentrations. This raised an important question. If the mechanism for antimicrobial activity requires permeabilizing the plasma membrane of the target organism, how can W_8-KIGAKI achieve high antimicrobial potency in light of its poor ability to induce membrane leakage?

To determine whether the properties of W_8-KIGAKI are common to other tryptophan analogues of KIGAKI, we also examined W_2-KIGAKI and W_{18}-KIGAKI. All three of these peptides possess the same amino acid content and are related to the parent compound by a single isoleucine-to-tryptophan substitution. Additionally, we examined a derivative of W_8-KIGAKI containing an octanoyl group at the amino terminus (Oct-W_8-KIGAKI). While these peptides are similar in antimicrobial activity (Table 2), they differ markedly in their ability to induce leakage in LUV (Figure 2). Oct-W_8-KIGAKI and, to a lesser extent, W_2-KIGAKI and W_{18}-KIGAKI promote significantly more leakage in POPC LUV and 4/1 POPC/POPG LUV than W_8-KIGAKI does. Thus, the amount of peptide bound and/or the behavior of the bound peptide must differ among these peptides. The low level of leakage induced by W_8-KIGAKI is not simply a result of a general isoleucine-to-tryptophan substitution, but is clearly position-specific.

All of these peptides were capable of inhibiting the growth of *E. coli* ML-35 (MIC = 2−4 μg/mL). We used this organism to compare the ability of the peptides to induce plasma membrane permeability by measuring the rate of entry of exogenous ONPG into the cytoplasm, where it is cleaved by constitutively produced β-galactosidase (Figure 3). At and above the MIC value, the α-helical peptides, KIAGKIA and W_9-KIAGKIA, were much better at promoting ONPG entry than the β-sheet peptides. Oct-W_8-KIGAKI and, to a lesser extent, W_2-KIGAKI and W_{18}-KIGAKI were more effective than KIGAKI or W_8-KIGAKI at inducing ONPG cleavage. W_8-KIGAKI was much less effective than the other peptides at 1 μg/mL (below the MIC values). In a comparison of the kinetics of bactericidal activity (Figure 8), there is a good correlation between the time scale of cell death and ONPG leakage. Thus, the extent of ONPG leakage measured in these experiments does not necessarily arise from a direct effect by the peptide on the plasma membrane. Even if cell death is induced by some means other than pore formation or direct membrane disruption by the peptides, a loss of integrity of the plasma membrane would be expected.

We used a method based on SPR spectroscopy to provide real-time kinetic data on peptide−lipid association and dissociation as a means of directly assessing peptide binding to lipid bilayers (*12*). Measurements were performed on KIGAKI and KIAGKIA using both 4/1 POPC/POPG and 4/1 POPE/POPG LUV. The selectivity differences observed previously between these peptides (*11*) were confirmed by the SPR results (Figure 6), with strikingly different binding preferences based upon the nature of the neutral phospholipid. A comparison of the affinity constants in Table 3 shows very strong binding for KIAGKIA with the PC-containing lipids and for KIGAKI with the PE-containing lipids. The binding by KIGAKI at a concentration of 50 μM to either lipid mixture was nearly irreversible. These observations are consistent with the lytic activity (Figure 1C,D) and induction of secondary structure (Figure 4C,D) in 4/1 POPC/POPG and 4/1 POPE/POPG LUV.

The secondary structure of these peptides was assessed using CD spectroscopy (Figures 4 and 5). No structure was

observed for any peptides in the presence of POPC LUV. As shown previously (*11*), KIGAKI and KIAGKIA adopted β-sheet and α-helical structure, respectively, in the presence of POPG LUV. The tryptophan-containing peptides exhibited structures similar to those of the parent compounds, but with decreased levels. KIAGKIA and W_9-KIAGKIA were partially α-helical in the presence of 4/1 POPC/POPG LUV, while KIGAKI and its tryptophan analogues were unstructured. The situation was reversed in the case of 4/1 POPE/POPG LUV, however, where the KIGAKI peptides exhibited some β-sheet structure. While CD data sometimes are used to estimate the level of peptide binding to lipid vesicles, it is not possible to distinguish between differences in the fraction of peptide bound and differences in the intrinsic conformation of bound peptides in these different lipid systems.

To gain better insight into the binding properties of the tryptophan-containing peptides, we used fluorescence spectroscopy to explore the interactions of W_9-KIAGKIA, W_2-KIGAKI, W_8-KIGAKI, Oct-W_8-KIGAKI, and W_{18}-KIGAKI with LUV with varying lipid compositions. If a peptide in aqueous solution binds to the bilayer surface, a shift to a lower frequency and an increase in intensity result if the polarity of the medium surrounding the tryptophan side chain is reduced. By measuring the change in fluorescence emission intensity, corrected for scattering effects, we estimated the binding parameters I_∞ and K_x using the method described by Ladhokin et al. (*16*). These fluorescence experiments confirmed the fact that the tryptophan-containing derivatives of KIGAKI interact differently with lipid vesicles than W_9-KIAGKIA does. In agreement with the CD results, no binding was detected for any of the peptides in the presence of POPC LUV. For POPG LUV, the I_∞ value of the latter peptide is much higher than those of the KIGAKI analogues (Table 4), suggesting that its tryptophan side chain resides in a more nonpolar environment when bound to vesicles. Moreover, W_9-KIAGKIA associates with POPG LUV to a greater extent than the KIGAKI peptides based upon their K_x values.

We also used this technique to compare peptide interactions with 4/1 POPC/POPG LUV and 4/1 POPE/POPG LUV. The most striking observation is that W_8-KIGAKI showed no discernible interactions with either of these lipid systems, although this peptide partitioned into POPG LUV to an extent similar to those of the other KIGAKI derivatives. Here again in these mixed lipid systems, W_9-KIAGKIA showed a much greater increase in intensity when bound. With the exception of W_8-KIGAKI, however, the remaining peptides demonstrated similar levels of binding (based upon K_x values) to 4/1 POPC/POPG LUV. With 4/1 POPE/POPG LUV, however, K_x for W_9-KIAGKIA was reduced by a factor of 3. For the KIGAKI-based peptides, the level of apparent binding of Oct-W_8-KIGAKI, W_2-KIGAKI, and, in particular, W_{18}-KIGAKI was much greater than that of W_9-KIAGKIA (Table 4). These results support the different lipid binding preferences of the β-sheet versus α-helical peptides observed by other techniques.

Many investigators studying antimicrobial peptides have used intrinsic fluorescence of tryptophan analogues as a tool to monitor their interactions with lipid surfaces (*5*, *13*, *18*−*22*). In most of these examples, tryptophan substitutions in these peptides were not expected to alter the fundamental nature of peptide−lipid interactions. Since tryptophan residues are known to prefer the interfacial region of membranes and lipid bilayers (*23*, *24*), however, the possibility that such substitutions might induce altered behavior cannot be dismissed. In the case of the α-helical peptide KIAGKIA, the isoleucine-to-tryptophan substitution does not appear to cause major changes in the ability of the peptide to interact with and permeabilize lipid bilayers. A similar substitution in the β-sheet peptide KIGAKI, however, results in considerably different properties with respect to lipid interactions. W_8-KIGAKI interacts strongly with lipid bilayers composed of POPG, as shown by tryptophan fluorescence (Figure 7). This peptide promotes calcein leakage from POPG LUV as effectively as KIGAKI (Figure 1B) and adopts β-sheet secondary structure upon binding to POPG LUV (Figure 3B).

In contrast, the differences between KIGAKI and W_8-KIGAKI are readily apparent in the mixed lipid systems composed of POPC and POPG, or POPE and POPG. In particular, W_8-KIGAKI binds much less avidly to and induces much less leakage in 4/1 POPE/POPG than KIGAKI does. Since this lipid composition is representative of the phospholipids in the *E. coli* plasma membrane, these observations bring into question whether W_8-KIGAKI exerts its antimicrobial activity solely as a membrane-lytic agent. A few antimicrobial peptides, such as drosocin and pyrrhocoricin, have been shown to function by binding to target proteins in a stereospecific manner (*25*, *26*). Most other antimicrobial peptides, particularly those for which the D-amino acid analogues possess equivalent potency, were thought to act by compromising the permeability barrier of the target cell.

Since all of the tryptophan analogues of KIGAKI possessed similar MIC values but appeared to differ in their ability to induce membrane leakage and bind to mixed lipid systems, we measured the kinetics of bactericidal action (Figure 8) in an attempt to reveal potential differences in the mechanism by which these peptides exert their lethal effects. In all cases, W_8-KIGAKI was the slowest to promote cell death, while Oct-W_8-KIGAKI was the fastest. The differences in killing times, however, were not sufficiently great that different mechanisms of action can be attributed to these peptides on the basis of these data alone.

Recent evidence, however, suggests that many antimicrobial peptides may not be capable of inducing lethal permeability changes in target plasma membranes at or near the MIC values (*27*−*29*). Thus, the molecular mechanisms of antimicrobial peptides may be more diverse and more complex than originally thought. The addition of an octanoyl group to the amino terminus of W_8-KIGAKI significantly enhanced the lytic potency and binding ability with mixed lipid LUV, but did not result in significantly improved antimicrobial activity. Moving the tryptophan in W_8-KIGAKI to either position 2 or 18 also resulted in greater interaction with mixed lipid LUV, but no gain in antimicrobial potency. The effects of a single tryptophan substitution for isoleucine appear to be functionally significant and position-dependent. In an effort to extend these studies, we plan to synthesize D-amino acid analogues of several of these peptides to differentiate between nonspecific and specific binding targets. We also will exploit SPR spectroscopy to probe differences in lipid binding among the tryptophan analogues of KIGAKI. A systematic investigation of a family of shorter amphipathic

β-sheet peptides as a function of tryptophan position is currently being carried out in an effort to gain a better understanding of the properties of this novel class of linear cationic antimicrobial peptides.

REFERENCES

1. Maloy, W. L., and Kari, U. P. (1995) *Biopolymers 37*, 105−122.
2. Tossi, A., Sandri, L., and Giangaspero, A. (2000) *Biopolymers 55*, 4−30.
3. Hancock, R. E. W., and Diamond, G. (2000) *Trends Microbiol. 8*, 402−410.
4. Chen, J., Falla, T. J., Liu, H. J., Hurst, M. A., Fujii, C. A., Mosca, D. A., Embree, J. R., Loury, D. J., Radel, P. A., Chang, C. C., Gu, L., and Fiddes, J. C. (2000) *Biopolymers 55*, 88−98.
5. Matsuzaki, K., Murase, O., Fujii, N., and Miyajima, K. (1995) *Biochemistry 34*, 6521−6526.
6. He, K., Ludtke, S. J., Huang, H. W., and Worcester, D. L. (1995) *Biochemistry 34*, 15614−15618.
7. Oren, Z., and Shai, Y. (1998) *Biopolymers 47*, 451−463.
8. Lehrer, R. I., Lichtenstein, A. K., and Ganz, T. (1993) *Annu. Rev. Immunol. 11*, 105−128.
9. Sokolov, Y., Mirzabekov, T., Martin, D. W., Lehrer, R. I., and Kagan, B. L. (1999) *Biochim. Biophys. Acta 1420*, 23−29.
10. Selsted, M. E., Novotny, M. J., Morris, W. L., Tang, Y.-Q., Smith, W., and Cullor, J. S. (1992) *J. Biol. Chem. 267*, 4292−4295.
11. Blazyk, J., Wiegand, R., Klein, J., Hammer, J., Epand, R. M., Epand, R. F., Maloy, W. L., and Kari, U. P. (2001) *J. Biol. Chem. 276*, 27899−27906.
12. Mozsolits, H., Wirth, H. J., Werkmeister, J., and Aguilar, M. I. (2001) *Biochim. Biophys. Acta 1512*, 64−76.
13. Breukink, E., Van Kraaij, C., Van Dalen, A., Demel, R. A., Siezen, R. J., De Kruijff, B., and Kuipers, O. P. (1998) *Biochemistry 37*, 8153−8162.
14. Chen, P. S., Toribara, T. Y., and Warner, H. (1956) *Anal. Chem. 28*, 1756−1758.
15. Skerlavaj, B., Romeo, D., and Gennaro, R. (1990) *Infect. Immun. 58*, 3724−3730.
16. Ladokhin, A. S., Jayasinghe, S., and White, S. H. (2000) *Anal. Biochem. 285*, 235−245.
17. Osterman, D. G., and Kaiser, E. T. (1985) *J. Cell. Biochem. 29*, 57−72.
18. Zhang, L. J., Benz, R., and Hancock, R. E. W. (1999) *Biochemistry 38*, 8102−8111.
19. Hong, J., Oren, Z., and Shai, Y. (1999) *Biochemistry 38*, 16963−16973.
20. Oh, D., Shin, S. Y., Lee, S., Kang, J. H., Kim, S. D., Ryu, P. D., Hahm, K. S., and Kim, Y. (2000) *Biochemistry 39*, 11855−11864.
21. Moll, G. N., Brul, S., Konings, W. N., and Driessen, A. J. M. (2000) *Biochemistry 39*, 11907−11912.
22. Dathe, M., Nikolenko, H., Meyer, J., Beyermann, M., and Bienert, M. (2001) *FEBS Lett. 501*, 146−150.
23. Wimley, W. C., and White, S. H. (1996) *Nat. Struct. Biol. 3*, 842−848.
24. Yau, W. M., Wimley, W. C., Gawrisch, K., and White, S. H. (1998) *Biochemistry 37*, 14713−14718.
25. Otvos, L., Jr. (2000) *J. Pept. Sci. 6*, 497−511.
26. Kragol, G., Lovas, S., Varadi, G., Condie, B. A., Hoffmann, R., and Otvos, L., Jr. (2001) *Biochemistry 40*, 3016−3026.
27. Wu, M. H., Maier, E., Benz, R., and Hancock, R. E. W. (1999) *Biochemistry 38*, 7235−7242.
28. Friedrich, C. L., Moyles, D., Beveridge, T. J., and Hancock, R. E. W. (2000) *Antimicrob. Agents Chemother. 44*, 2086−2092.
29. Koo, S. P., Bayer, A. S., and Yeaman, M. R. (2001) *Infect. Immun. 69*, 4916−4922.

BI034338S